JETIR.ORG ISSN: 2349-5162 | ESTD Year : 2014 | Monthly Issue
JOURNAL OF EMERGING TECHNOLOGIES AND INNOVATIVE RESEARCH (JETIR)
An International Scholarly Open Access, Peer-reviewed, Refereed Journal

Enhancing Photovoltaic Performance of TiO_2/CuO Nanocomposite through CuO Nanoparticle and Dye-Loading Concentration

Savita Rambhau Nemade, Purnima Swarup Khare

Department of School of Nanotechnology, Rajiv Gandhi Prodyogiki Vishwavidyalaya (RGPV) Bhopal, State Technological University, 462033, India.

Abstract : The aim of this research was to investigate the influence of three key factors on photovoltaic (PV) cell performance: the concentration of CuO nanoparticles in TiO_2-CuO nanocomposites, the loading concentration of N3 dye, and the loading time of N3 dye. These factors were found to significantly affect PV cell performance. The study utilized an ex-situ approach to prepare the necessary nanocomposites, which were then characterized using various techniques such as X-ray diffraction (XRD), scanning electron microscopy (SEM), Fourier-transform infrared spectroscopy (FTIR), ultraviolet-visible (UV-VIS) spectroscopy, and photoluminescence (PL) spectroscopy. PV cell performance was evaluated through analysis of its current-voltage characteristics and assessment of parameters including short circuit current, open circuit voltage, fill factor, and power conversion efficiency. Optimization revealed that a dye-sensitized solar cell (DSSC) comprising a 20 wt.% CuO loaded TiO_2 nanocomposite, with a 3% N3 dye loading concentration and a 2-hour dye loading time, exhibited the highest power conversion efficiency, reaching 5.273%.

Index Terms **- CuO, TiO_2, Nanocomposite, Photovoltaic Application**

I. INTRODUCTION

Conventional fossil fuel production has numerous negative impacts on the environment, including the generation of acid rain, contributing to global warming, and causing pollution. In contrast, renewable energy sources offer a more positive environmental impact. One popular form of renewable energy is thin film solar cells. As technology advances, energy production becomes increasingly crucial. Currently, electricity generation heavily relies on the combustion of fossil fuels. However, there is a growing need to exploit renewable energy sources sustainably and simultaneously reduce pollutant emissions in both air and water. This necessitates the development of new technologies that utilize efficient, abundant, low-toxicity, and cost-effective materials. Photoelectrochemical devices that utilize abundant elements as photoelectrodes show promise in harnessing solar energy [1].

The oxides of transition metals are an important class of semiconductors and have been studied because of their special properties for potential applications like solar cells, electronics and photocatalyst. Transition metal oxides are useful in Dye-Sensitized Solar Cell (DSSC) applications due to several key characteristics such as their excellent optoelectronic properties, electron transport, transparent conductivity, stability, and compatibility with various organic dyes [2]. Transition metal oxides, such as titanium dioxide (TiO_2), zinc oxide (ZnO) and copper oxide (CuO) have desirable optoelectronic characteristics. These metal oxides have wide bandgaps, allowing them to absorb a significant portion of the solar spectrum. This absorption enables efficient conversion of light energy into electrical energy. Similarly, the transition metal oxides possess excellent electron transport characteristics. When light is absorbed by the oxide, it generates excited electrons. These electrons can efficiently move through the oxide material due to its unique electronic structure, facilitating the flow of electrical current [3]. Few transition metal oxides, like indium tin oxide (ITO) and fluorine-doped tin oxide (FTO) possesses both electrical conductivity and optical transparency. This combination is very useful in photovoltaic cells as it allows light to pass through the transparent conducting oxide while also facilitating the collection and transport of generated electrons [4]. Another important characteristic associated with transition metal oxides is that they are chemically stable and resistant to environmental degradation. This stability is important for the long-term performance and durability of solar cells, ensuring their functionality over an extended period. Finally, the compatibility of transition metal oxides with organic dyes is also play crucial role in solar cell application. The oxide layer serves as the electron acceptor and transporter, interacting with the dye molecules to facilitate electron transfer and conversion of light into electricity [5].

CuO and TiO_2 are promising materials for photovoltaic applications, primarily due to their non-toxicity and cost-effectiveness. These materials offer advantages in terms of environmental friendliness as well as economic feasibility. Copper and titanium are abundant in nature, and their production methods are straightforward and inexpensive. Additionally, DSSCs have gained significant attention in the field of solar cells due to their low cost, high stability, and high efficiency. In conventional DSSCs, a mesoporous film comprising nanocrystalline TiO_2 is used, which provides a large surface area for enhanced dye adsorption and facilitates the diffusion of electrolytes [6].

Several studied are reported in literature, which shows that TiO_2 and CuO based composite shows considerable power conversion efficiency. This category of material system needs systematic approach of study that optimized power conversion efficiency.
Here is a literature review focusing on dye-sensitized solar cells (DSSCs) utilizing TiO2-CuO nanocomposites for photovoltaic purposes. CuO and TiO_2 nanoparticles were synthesized using the hydrothermal method by Abdulnabi et al. They also prepared a composite of CuO/TiO_2 nanocomposites by combining them in equal proportions (1:1) using the hydrothermal technique. Subsequently, DSSCs were fabricated using CuO/TiO_2 nanocomposites, with FTO as the front electrode and a carbon/FTO-glass substrate as the back electrode. The research findings indicate that the CuO/TiO_2 nanocomposites, sensitized with chlorophyll pigment from green leek, demonstrated a power conversion efficiency of approximately 1.51% [7]. Rokhmat et al conducted a study where they developed a solar cell based on a TiO_2/CuO/Cu/PVA.LiOH/Al structure. They achieved the growth of copper particles in the space between TiO2 and CuO particles. In their experimental setup, a TiO_2/CuO film was fabricated by utilizing a spraying process to deposit a TiO_2/CuO suspension onto an FTO (Fluorine-doped Tin Oxide) substrate. The copper particles were then grown through fixed current electroplating. The prepared photovoltaic (PV) cell demonstrated the highest power conversion efficiency of 1.62% and a fill factor of 0.42 [8]. Martinez et al conducted a study on the photovoltaic characteristics of a TiO_2/CuO system modified with N719 (ruthenium (II) ammonium bistetrabutyl) as a sensitizer. The results of their study revealed a power conversion efficiency of 2% [9]. Narasimman et al conducted a study where they prepared and analyzed Dye-Sensitized Solar Cells (DSSCs) using natural dyes such as raspberries and pomegranates, along with different cathode electrode plates including carbon and graphite. The active material used in this study was a TiO2-CuO nanocomposite. The research findings suggest that the incorporation of CuO with TiO2 reduces the bandgap of the semiconductor, leading to an increase in the power conversion efficiency of 6.87% [10]. Shah et al conducted a study where they proposed methods to mitigate electron recombination from TiO_2 to the oxidized dye in Dye-Sensitized Solar Cells (DSSCs). They achieved this by incorporating copper nanopowder as an electron recombination barrier within the TiO2 layer. The DSSC containing 3 wt% of copper nanopowder exhibited a power conversion efficiency of 7.19% [11].
Throughout the existing literature, several studies have reported significant power conversion efficiency achieved by utilizing composite materials based on TiO_2 and CuO for DSSCs. However, there is a need for further research to systematically investigate and optimize the power conversion efficiency of this material system. During the literature survey, it becomes evident that there is a significant scope for optimizing the photovoltaic performance of TiO_2-CuO-based DSSCs. The existing literature lacks comprehensive studies that explore the effects of CuO nanoparticle concentration, dye loading concentration, and time on the performance of TiO_2-CuO-based DSSCs. Therefore, conducting thorough investigations in these areas would contribute to a more comprehensive understanding and advancement of TiO_2-CuO-based DSSCs for enhanced photovoltaic performance.
Following reasons motivate us to study DSSC based on TiO_2-CuO nanocomposites,

- The addition of CuO into TiO_2 can lead to improved power conversion efficiency, because the CuO acts as an electron recombination barrier, reducing the loss of photo-generated electrons and enhancing the overall power conversion efficiency of cell.
- The synergetic state of TiO_2 and CuO can potentially broaden the absorption range of the DSSC. This expanded absorption range allows for better utilization of a wider range of solar wavelengths, leading to increased light harvesting and improved efficiency.
- TiO_2-CuO nanocomposite promotes efficient charge separation and transport within the DSSC. The incorporation of CuO nanoparticles enhances the electron transport properties and reduces recombination losses, leading to improved charge collection efficiency.
- Both TiO_2 and CuO are relatively low-cost materials, readily available in abundance. This makes TiO_2-CuO-based DSSCs an attractive option from a cost perspective, making them more economically viable for large-scale photovoltaic applications.
- TiO_2 and CuO are non-toxic materials, making them environmentally friendly choices for photovoltaic applications. The use of these materials reduces the potential ecological impact associated with the manufacturing and disposal of solar cells.

The aim of the present study was to investigate the Dye-Sensitized Solar Cell (DSSC) characteristics of a TiO_2-CuO-based photovoltaic cell sensitized with N3-ruthenium dye. The research focused on analyzing the influence of CuO concentration on the performance of various photovoltaic parameters. Additionally, the effects of N3-ruthenium dye loading concentration and time were evaluated to optimize the power conversion efficiency of the TiO_2-CuO-based DSSC. By examining these factors, the study aimed to enhance the overall performance of the DSSC and improve its efficiency as a photovoltaic device.

II. Experimental

All chemicals and reagents used in this study was purchased from SD Fine, India sources. To prepare the TiO_2 nanoparticles, the following procedure was adopted. First, in a beaker 10 ml of titanium isopropoxide ($C_{12}H_{28}O_4Ti$) was combined with 20 ml of ethanol. The beaker containing the mixture was placed under magnetic stirring for 30 minutes. Aqueous ethanol solution was then added dropwise into the titanium isopropoxide solution while continuing the magnetic stirring. This process was carried out for 1 hour. The resulting solution was heated to 100 °C and maintained at this temperature for 6 hours. After the heating step, the solution was washed with water and ethanol to remove impurities. The washed precipitate was dried overnight at 50 °C to ensure complete removal of any remaining moisture. The dried precipitate was collected and subjected to calcination at 60 °C for 5 hours. This calcination process aids in the stabilization of TiO_2 nanoparticles. By implementing these steps, TiO_2 nanoparticles was prepared successfully.
In a separate beaker, 5 g of KOH was combined with 30 ml of ethanol and subjected to magnetic stirring for 30 minutes. In another beaker, 0.5 g of copper acetate ($Cu(CH_3COO)_2$) was mixed with 150 ml of ethanol. Both solutions were subjected to ultrasonication at room temperature for one hour to ensure proper dispersion of the compounds. The KOH solution was then added dropwise to the copper acetate solution. The resulting mixture was subjected to magnetic stirring for 1 hour to promote the reaction between the compounds, facilitating the formation of CuO nanoparticles. The CuO nanoparticles were obtained as a precipitate. The final solution was washed with additional ethanol, repeating the process multiple times to remove impurities. The

washed solution was then placed in an oven at 60 °C for drying. By following the above-mentioned methodology, CuO nanoparticles were successfully prepared.

In this study, an ex-situ approach was employed to prepare composites. The composites were formed by incorporating CuO nanoparticles into TiO_2 nanoparticles, with the weight percent (wt.%) stoichiometry. Specifically, five composite samples were prepared by introducing varying concentrations of CuO nanoparticles into TiO2 nanoparticles, ranging from 5 wt.% to 25 wt.% in increments of 5 wt.%. The wt.% stoichiometry was calculated using equation 1,

$$wt.\% = \frac{X}{(X+Y)} \times 100 \quad (1)$$

where X (CuO) and Y (TiO_2) are constituents of composite. To prepare a 5 wt.% CuO loaded TiO_2 nanocomposite, the following procedure was followed. Similarly, the same methodology was employed for the preparation of other composite systems with different CuO concentrations:

- The required quantity of CuO nanoparticles was taken in a beaker containing 30 ml of ethanol and subjected to magnetic stirring for 30 minutes.
- Simultaneously, TiO_2 nanoparticles were taken in a separate beaker containing 30 ml of ethanol and subjected to magnetic stirring for 30 minutes as well.
- After the magnetic stirring, the suspension containing CuO nanoparticles was added dropwise to the TiO_2 nanoparticle suspension under continued magnetic stirring.
- The resulting suspension was further stirred magnetically for 1 hour.
- Subsequently, the suspension was heated at 60 °C for drying.
- This process resulted in the preparation of the 5 wt.% CuO loaded TiO_2 nanocomposite.
- The same methodology was applied to prepare the remaining composite systems: 10 wt.%, 15 wt.%, 20 wt.%, and 25 wt.% CuO loaded TiO_2 nanocomposites.

To differentiate these composites, they were labeled as 5TC, 10TC, 15TC, 20TC, and 25TC for convenience. By following these steps, CuO loaded TiO_2 nanocomposites with different wt.% of CuO were successfully prepared.

The structural analysis of both the pure and nanocomposite materials was conducted utilizing the X-ray diffraction (XRD) technique. XRD measurements were performed using a Rigaku Miniflex-XRD instrument with an X-ray wavelength of 1.5406 Å. The morphological analysis of the nanocomposites was carried out using a scanning electron microscope (SEM) with a ZEISS SIGMA model instrument. The SEM operated at an acceleration voltage of 5 kV. For examining the elemental distribution, energy dispersive X-ray analysis (EDAX) was performed using an EAG AN461 instrument. The Fourier-transform infrared spectroscopy (FTIR) spectra of the nanocomposites were obtained using a BRUKER ALPHA Platinum ATR-IR instrument. To investigate the optical characteristics of the nanocomposites, ultraviolet-visible (UV-VIS) absorption spectra were recorded using an Agilent Cary 60 UV-VIS spectrophotometer. Furthermore, the photoluminescence (PL) spectra of the nanocomposites were measured using an FL Spectrophotometer with the model HITACHI F-7000. In summary, XRD, SEM, EDAX, FTIR, UV-VIS, and PL techniques were employed for the structural, morphological, elemental, infrared, optical, and photoluminescence analyses of the pure and nanocomposite materials.

The doctor blade technique was used to construct the photovoltaic (PV) cells [12]. In this process, a nanocomposite material was positioned between a cleaned ITO plate, serving as the transparent electrode, and an aluminum foil, which served as the metallic electrode in the PV cell architecture. The ITO plate used in this study was sourced from Techinstro (ITO-SE-011), India, and had dimensions of 25mm×25mm. To aid the deposition of the nanocomposite onto the ITO electrode, a temporary binder was employed. This temporary binder was prepared using a mixture of 3% ethyl cellulose and 97% butyl digol. The active nanocomposite material investigated in this study maintained a consistent thickness of approximately 100 microns. After the fabrication process, the PV cell was allowed to dry at 50 °C for 1 hour to promote the evaporation of volatile organic compounds present in the composite material. The dimensions and other pertinent details of the PV cell are illustrated in Figure 1. Before conducting PV cell testing, the nanocomposite layer within the PV cell was sensitized with a ruthenium-based red dye (N3). This sensitization process was achieved through capillary action, with the nanocomposite being exposed to the N3 dye for 1 hour.

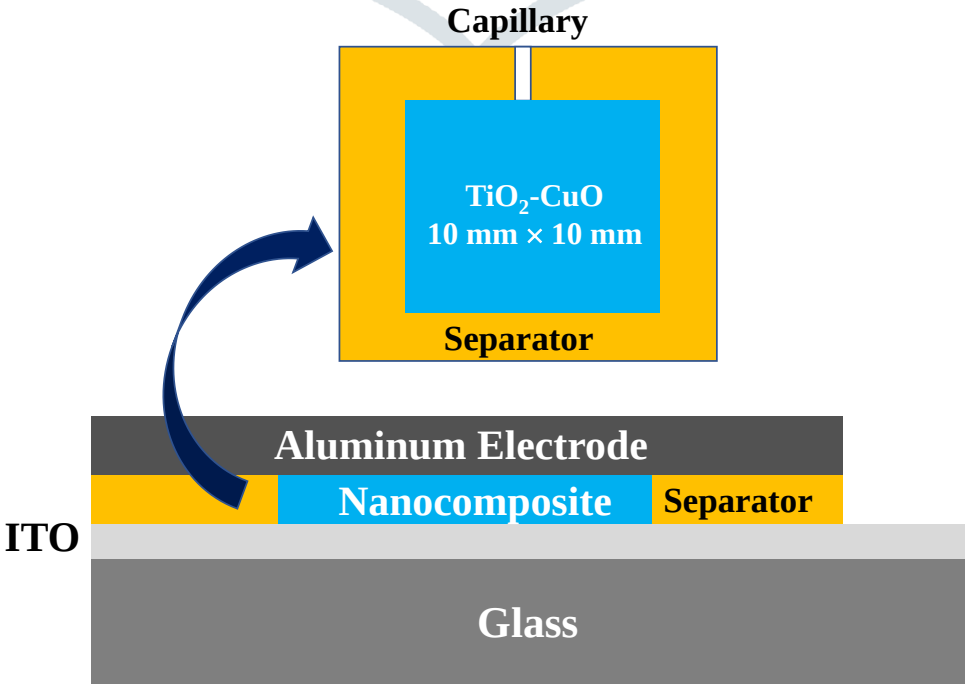

Figure 1. The architectural illustration of the PV Cell.

The current-voltage measurements were conducted using a Keithley 2400 source/meter under the control of a PC. The measurements were taken while irradiating the samples at 100 mW/cm^2 using a solar simulator (Newport 91160) that simulated AM 1.5G sunlight. In the mentioned conditions, important diode parameters such as open circuit voltage (V_{OC}), short circuit current (I_{SC}), fill factor (FF), and power conversion efficiency (η) were determined. The FF of PV cell computed using equation (2) [13],

$$FF = \frac{I_{MAX} \times V_{MAX}}{I_{SC} \times V_{OC}} \quad (2)$$

whereas, power conversion efficiency (%η) of PV cell were calculated using the equation (3),

$$\%\eta = \left(\frac{I_{SC} \times V_{OC} \times FF}{P_{in}} \right) \times 100 \quad (3)$$

where, P_{in} is power incidence.

III. Results and Discussion

Figure 2 (a) shows the XRD pattern of anatase TiO_2 exhibits the distinct peaks in its XRD pattern. For anatase TiO_2, the prominent peaks are commonly observed around 25.3°, 37.8°, 48.1°, 54.1°, 62.7°, and 75.0°. The peak positions in the XRD pattern can be related to the crystallographic planes of anatase TiO_2 using Miller indices. The most intense peak, often observed at around 25.3° (2θ position), corresponds to the (101) crystal plane of anatase TiO_2. Similarly, other peaks at 37.8°, 48.1°, 54.1°, 62.7° and 75.0° assigned to the (004), (200), (105), (211), and (204) crystal planes, respectively.

Figure 2 (b) illustrates the XRD pattern of CuO, displaying distinct and intense peaks at specific 2θ values. The positions of the observed sharp diffraction peaks at 2θ = (32.59°, 35.61°, 38.78°, 48.82°, 53.54°, 58.37°, 61.60°, 66.31°, and 68.15°) were assigned to the crystallographic planes (110), (−111), (111), (−202), (020), (202), (−113), (−311), and (220), respectively. These assignments are in excellent agreement with the JCPDS standard no. 01-080-0076, which describes the XRD pattern of CuO nanoparticles with a monoclinic phase.

Figure 2 (c-g) shows the XRD pattern of TiO_2-CuO nanocomposites (5TC, 10TC, 15TC, 20TC and 25TC systems). The XRD pattern of a TiO_2-CuO nanocomposite gives insights into the crystal structures and phases present in the material. The XRD pattern of a TiO_2-CuO composite will typically show characteristic peaks associated with both TiO_2 and CuO. XRD pattern shows some peaks from TiO_2 and CuO which overlap or interfere with each other. This make it challenging to distinguish individual contributions from each phase based solely on peak positions. In addition to this, the XRD pattern of a TiO_2-CuO composite shows minor shifting in peaks, indicating the formation of composite phases. This results from the interactions between TiO_2 and CuO, leading to structural modifications. Further, XRD pattern of TiO_2-CuO nanocomposites shows slight peak broadening effect. It is attributed to the increased concentrations of CuO in the nanocomposite. The increased concentration of CuO nanoparticles results into lattice strain and the introduction of defects. This lattice strain cause peak broadening, as the lattice becomes distorted [14].

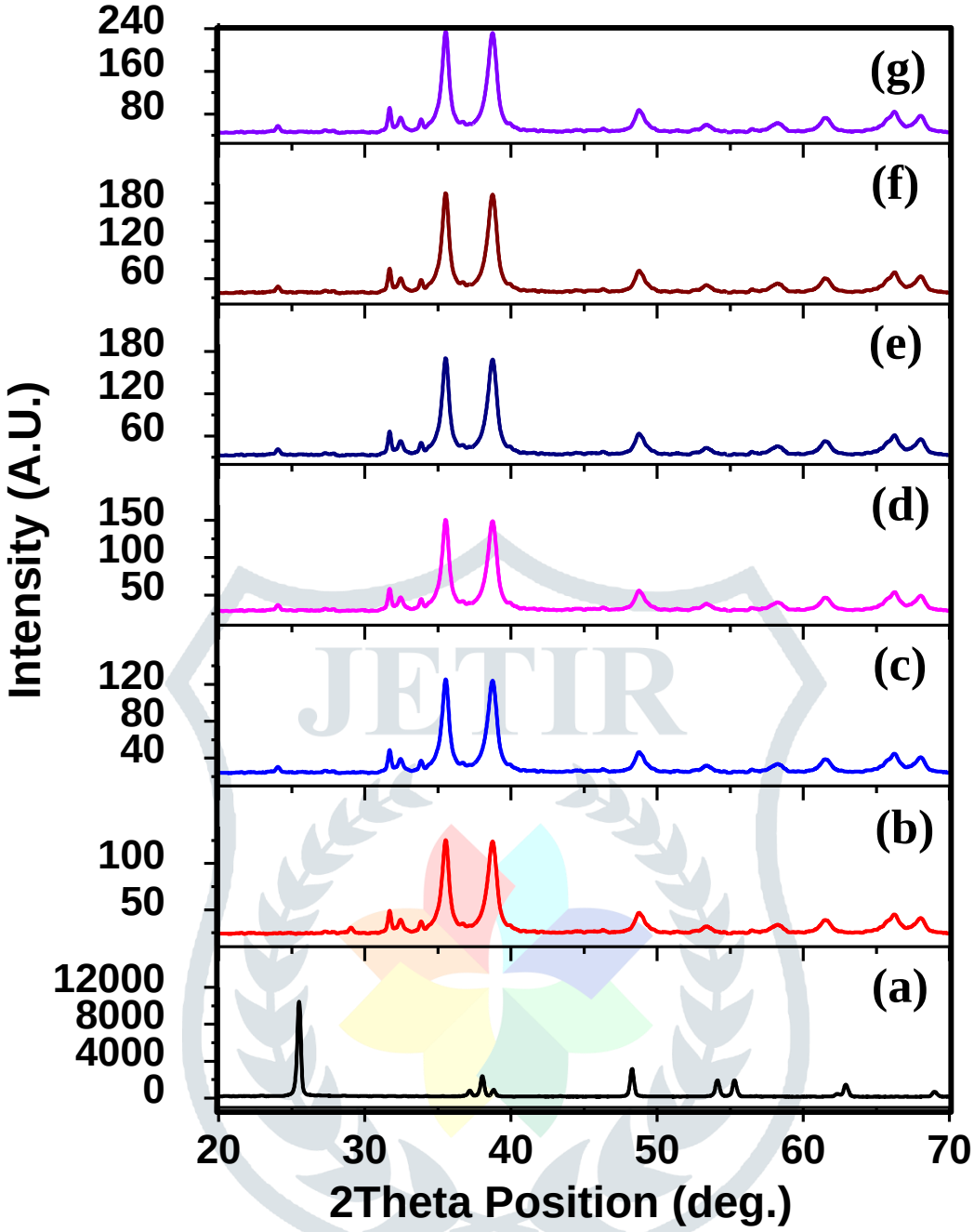

Figure 2. XRD Pattern of (a) TiO_2, (b) CuO, (c) 5TC, (d) 10TC, (e) 15TC, (f) 20TC and (g) 25TC systems.

SEM analysis was utilized to investigate the morphological characteristics of a TiO_2-CuO nanocomposite by visually examining the surface of the nanocomposites. The SEM images in Figure 3 (a-e) depict the 5TC, 10TC, 15TC, 20TC, and 25TC systems respectively, while Figure 3 (f) illustrates the EDX elemental mapping of the 20TC system. All SEM images of the nanocomposite exhibit a flake-like morphology, with some minor agglomeration observed in the composites. The average particle size, as determined from the SEM images, ranges from 89 nm to 94 nm for the TiO_2-CuO nanocomposite. This data provides a comprehensive understanding of the composite and its microstructure, facilitating the optimization of its properties for photovoltaic (PV) cell applications. The EDX elemental mapping of the TiO_2-CuO composite in Figure 3 (f) offers valuable insights into the spatial distribution of elements within the composite material. The EDX analysis clearly reveals the distribution of titanium (Ti), oxygen (O), and copper (Cu) within the nanocomposite. Furthermore, the uniform distribution of Ti and Cu indicates a well-mixed composition and potential interaction between the materials.

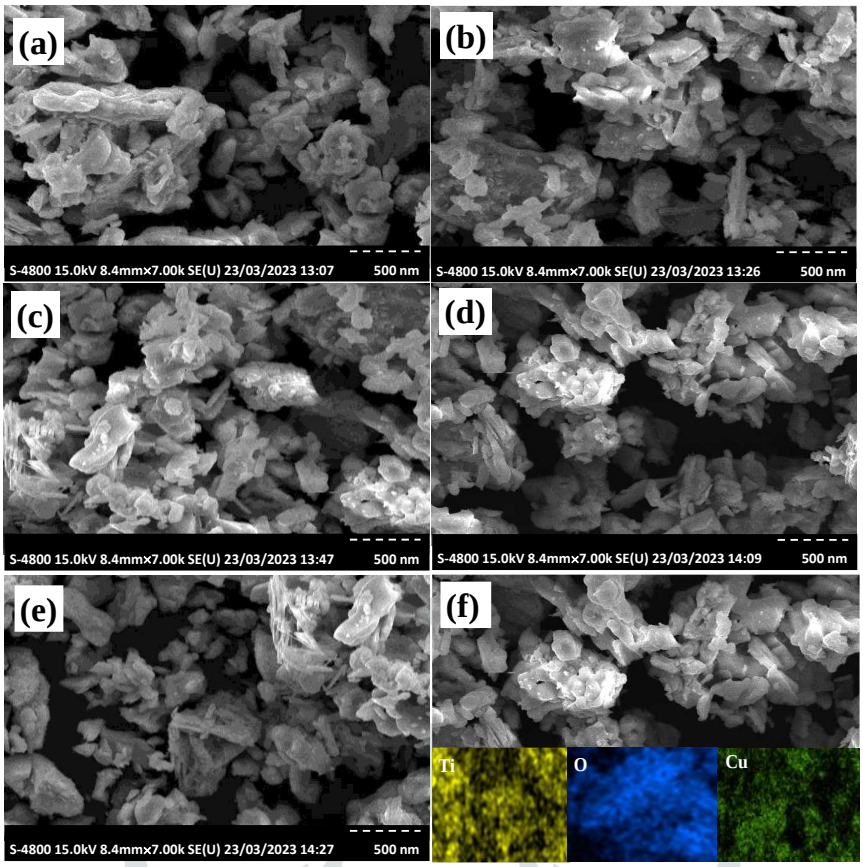

Figure 3. SEM images of (a) 5TC, (b) 10TC, (c) 15TC, (d) 20TC, (e) 25TC systems and (e) EDX elemental mapping of 20TC system (Optimized system in PV study).

Fourier transform infrared (FTIR) spectrometry was employed to investigate the formation of metal-oxygen bonds in the TiO_2-CuO nanocomposite. Figure 4 (a-e) presents the FTIR spectra of the nanocomposite, which was prepared by varying the weight percentage (wt.%) concentration of CuO nanoparticles in the composite. The FTIR analysis revealed similar results for all TiO_2-CuO nanocomposites. An absorption band at approximately 3400 cm^{-1} was observed, indicating O-H stretching vibrations. In the vicinity of 2900 cm^{-1}, a weak absorption band was detected, attributed to CO_2. A C-C band was observed around 1600 cm^{-1}. Additionally, a very weak absorption band in the range of 1100-1400 cm^{-1} indicated C-H stretching vibrations. The presence of Ti-O-Ti stretching bands was confirmed at 770 and 800 cm^{-1}. A strong stretching band for Cu-O was observed around 600 cm^{-1} [15]. Consequently, FTIR spectroscopy provided confirmation of the formation of the TiO2-CuO nanocomposite. These results were further supported by XRD and EDX analyses.

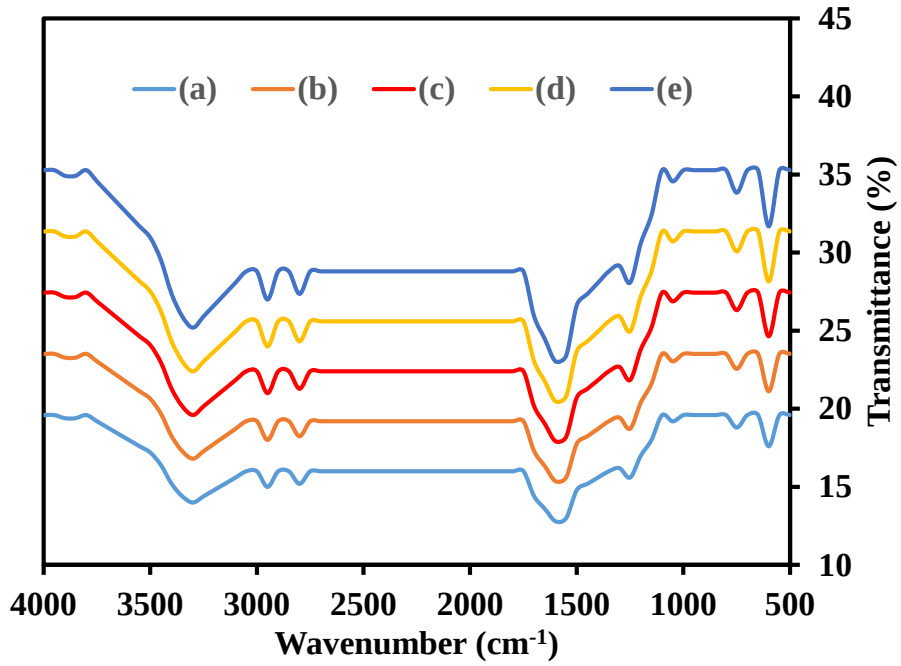

Figure 4. FTIR spectra of (a) 5TC, (b) 10TC, (c) 15TC, (d) 20TC and (e) 25TC systems.

The UV-VIS spectroscopy results of the nanocomposite systems, namely 5TC, 10TC, 15TC, 20TC, and 25TC, are depicted in Figure 5 (a-e). These spectroscopic measurements provide important insights into the optical properties and bandgap energy of the nanocomposites, indicating their potential applications in photovoltaic cells. Generally, TiO_2 and CuO nanoparticles exhibit

strong absorption in the ultraviolet (UV) region. TiO_2 shows absorption within the range of 320-400 nm [16], while CuO exhibits absorption between 200-300 nm [17]. In the present study, the TiO_2-CuO nanocomposites displayed absorption wavelengths as listed in Table 2. Analysis of Table 1 reveals that the optical bandgap value decreases with an increase in the weight percentage (wt.%) of CuO in the TiO_2-CuO nanocomposite. In other words, the concentration of CuO nanoparticles influences the optical bandgap of the TiO_2-CuO nanocomposites. The incorporation of CuO in the composite material alters its electronic structure and bandgap. The energy levels of CuO nanoparticles interact with TiO_2 nanoparticles, resulting in changes to the band structure and optical properties. Understanding the relationship between the concentration of CuO and the optical bandgap in TiO_2-CuO nanocomposites is crucial for tailoring their optical properties specifically for photovoltaic applications.

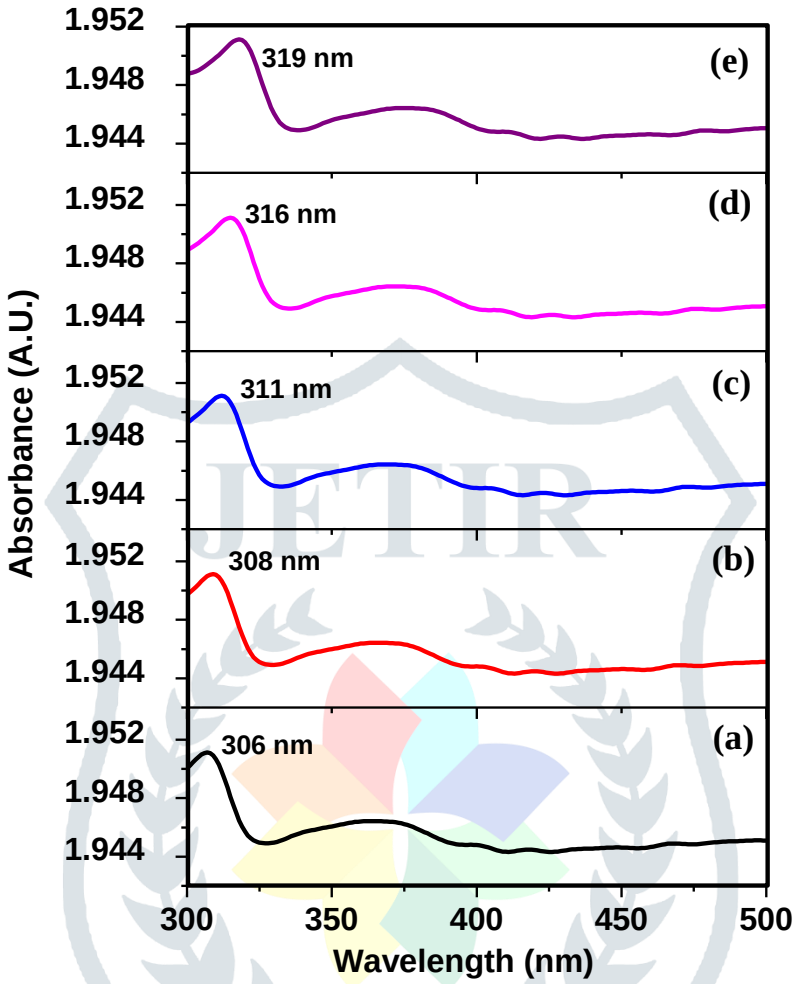

Figure 5. UV-Vis spectra of (a) 5TC, (b) 10TC, (c) 15TC, (d) 20TC and (e) 25TC systems.

Table 1. Absorption wavelength and optical band gap of 5TC, 10TC, 15TC, 20TC and 25TC nanocomposite systems.

Sample	Absorption Wavelength (nm)	Optical Band Gap (eV)
5TC	306	4.051
10TC	308	4.025
15TC	311	3.986
20TC	316	3.923
25TC	319	3.886

Figure 6 (a-e) presents the photoluminescence (PL) spectra of the 5TC, 10TC, 15TC, 20TC, and 25TC systems, respectively. The PL analysis offers valuable insights into the suitability of TiO_2-CuO nanocomposites for photovoltaic applications. The PL spectra of the TiO_2-CuO composites exhibit emission peaks at a wavelength of 395 nm when excited at a wavelength of 325 nm at room temperature. It is noteworthy that the PL intensity decreases significantly with increasing concentration of CuO nanoparticles in the TiO_2-CuO nanocomposite system. Generally, CuO exhibits a higher concentration of defect states compared to TiO2. Therefore, the incorporation of CuO into the TiO_2 matrix leads to an increased concentration of defect states, which can contribute to enhanced non-radiative recombination processes, resulting in a reduction of the overall PL intensity [18].

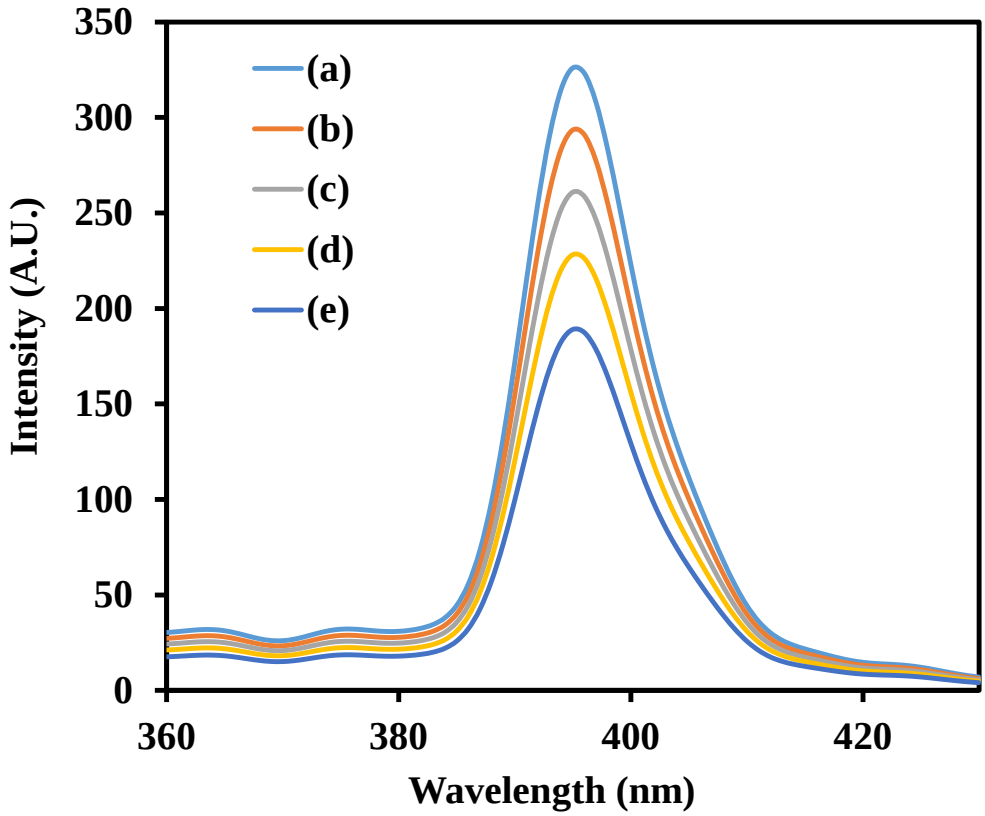

Figure 6. PL spectra of (a) 5TC, (b) 10TC, (c) 15TC, (d) 20TC and (e) 25TC systems.

Figure 7 (a-e) illustrates the current-voltage (I-V) characteristics of DSSCs based on different concentrations of CuO, namely 5TC, 10TC, 15TC, 20TC, and 25TC. The relevant PV cell parameters are provided in Table 3. The as-fabricated PV cells demonstrate stable photovoltaic performance, which means they exhibit consistent readings over time with minimal deviation. The data presented for the I-V characteristics represents the average of five sets of readings, collected at hourly intervals. These readings exhibit negligible variation. According to Table 2, the DSSC based on a 20 wt.% concentration of CuO (referred to as the 20TC system) exhibits the highest power conversion efficiency. This system showcases the following values: Imax = 1.609 mA, Vmax = 0.4 V, Isc = 1.653 mA, Voc = 0.8 V, FF = 0.3115, and η% = 4.120. The power conversion efficiency increases with an increment of 5 wt.% concentration of CuO in the TiO_2-CuO nanocomposite system, up to the 20 wt.% level. However, beyond the 20 wt.% concentration of CuO, the power conversion efficiency declines. This decrease in efficiency beyond a certain concentration of CuO in the TiO_2-CuO nanocomposite system can be attributed to four primary factors: Charge Transport and Recombination, Electron Diffusion Length, Light Harvesting and Dye Loading, and Charge Transfer Resistance.

The inclusion of CuO nanoparticles in TiO_2 nanoparticles affects the charge transport and recombination processes within the DSSC. While a small amount of CuO can enhance charge transport and reduce recombination, an excessive concentration of CuO can lead to increased charge recombination and hinder the transport of charge carriers, ultimately diminishing the overall efficiency. Similarly, the addition of CuO nanoparticles to TiO_2 nanoparticles can influence the electron diffusion length within the composite system. At lower concentrations, CuO nanoparticles can improve the electron diffusion length and enhance the collection of photogenerated electrons. However, higher concentrations of CuO particles may form aggregates or create defects that restrict electron diffusion, resulting in a decrease in power conversion efficiency [19].

Furthermore, the incorporation of CuO nanoparticles into TiO_2 nanoparticles may impact the light harvesting capability and dye loading capacity of the DSSC. At fixed concentrations, CuO particles can impede light absorption, leading to a reduction in the number of photons converted into charge carriers and a decrease in overall power conversion efficiency. Higher concentrations of CuO also lead to an increase in interfacial charge transfer resistance between the material system and the electrolyte in the DSSC. This elevated resistance hampers the efficient transfer of charge carriers across the interface, consequently lowering the power conversion efficiency [20, 21].

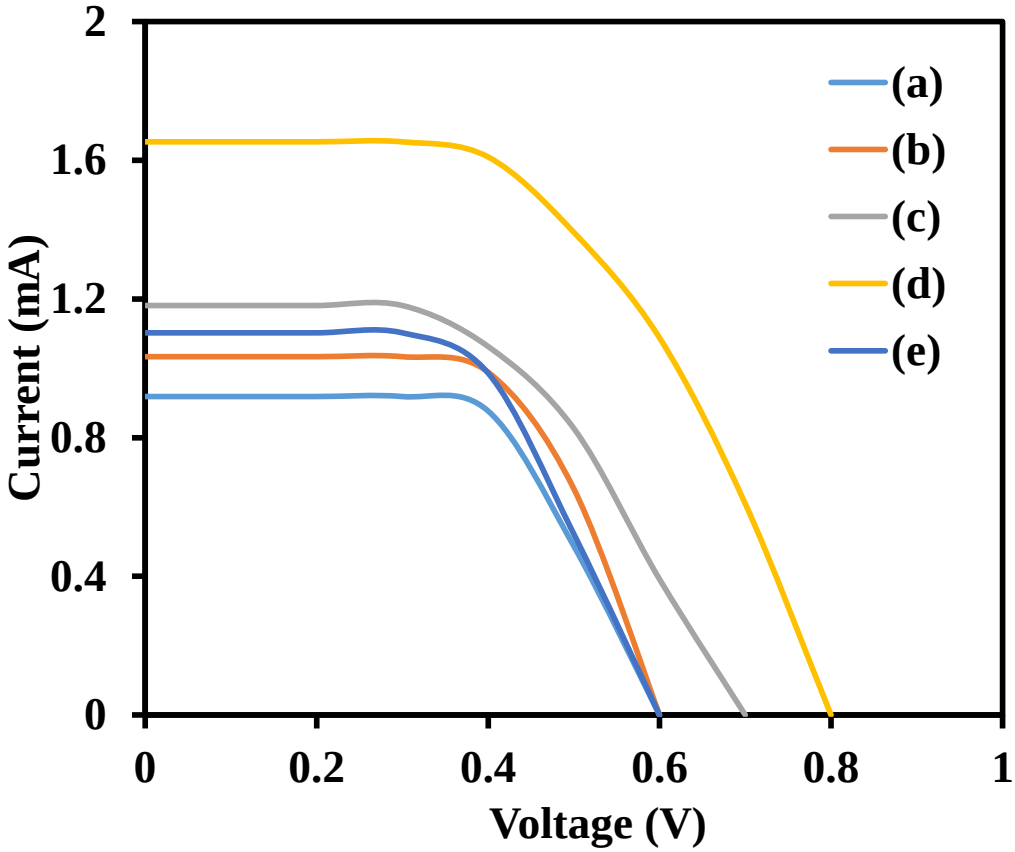

Figure 7. I-V characteristics of (a) 5TC, (b) 10TC, (c) 15TC, (d) 20TC and (e) 25TC based PV cells.

Table 2. PV parameters of 5TC, 10TC, 15TC, 20TC and 25TC based PV cells.

Sample	Imax (mA)	Vmax (V)	Isc (mA)	Voc (V)	FF	η(%)
5TC	0.876	0.4	0.918	0.6	0.2291	1.262
10TC	0.988	0.4	1.033	0.6	0.2296	1.423
15TC	1.062	0.4	1.180	0.7	0.2519	2.082
20TC	1.609	0.4	1.653	0.8	0.3115	4.120
25TC	0.986	0.4	1.102	0.6	0.2147	1.419

Figure 8 (a-e) presents the current-voltage characteristics of N3 dye-sensitized DSSC devices with different dye loading concentrations: 1%, 2%, 3%, 4%, and 5%. These devices were fabricated for one hour to investigate the impact of dye-loading concentration on charge injection. The power conversion efficiency of DSSCs is influenced by multiple factors, including the dye loading concentration. In this study, the effect of dye loading concentration is examined using N3 dye, which is a ruthenium-based sensitizer. The dye loading concentration refers to the amount of dye molecules adsorbed onto the surface of the materials under investigation. This adsorption of dye molecules plays a crucial role in key parameters such as light absorption efficiency, charge generation, and charge transport within the DSSC.

In the case of the 20TC-based DSSC sensitized by N3 dye with a loading concentration of 3%, the PV parameters indicate the highest power conversion efficiency of approximately 4.794% with an FF value close to 0.3115 (refer to Table 3). It is observed that the PV performance of cells begins to decline for concentrations higher than 3%. This behaviour of the 20TC-based DSSC sensitized by N3 dye with loading concentrations ranging from 1% to 5% can be attributed to an increase in the dye loading concentration, which generally leads to enhanced light absorption in the visible spectrum. This is because a higher concentration of dye molecules allows for more efficient harvesting of incident light. As a result, more light energy is absorbed by the dye, leading to a higher power conversion efficiency. Additionally, the dye molecules are responsible for absorbing photons and generating electron-hole pairs (excitons). These excitons are subsequently separated into free electrons and holes, facilitating charge generation. An optimal dye loading concentration ensures an adequate number of dye molecules for efficient light absorption and charge generation, thereby maximizing the power conversion efficiency.

However, excessive dye loading concentration also affects charge transport within the DSSC. An excessively high concentration of dye loading may cause clustering of dye molecules, impeding efficient electron transport through the TiO_2-CuO layer. At higher dye loading concentrations, there is a greater likelihood of dye aggregation on the TiO_2-CuO surface. Dye aggregation can lead to self-quenching, where the absorbed light energy is dissipated as heat instead of being utilized for charge generation, ultimately resulting in a decrease in power conversion efficiency [22, 23]. Therefore, determining the optimal dye loading concentration is an essential step in the study of DSSCs.

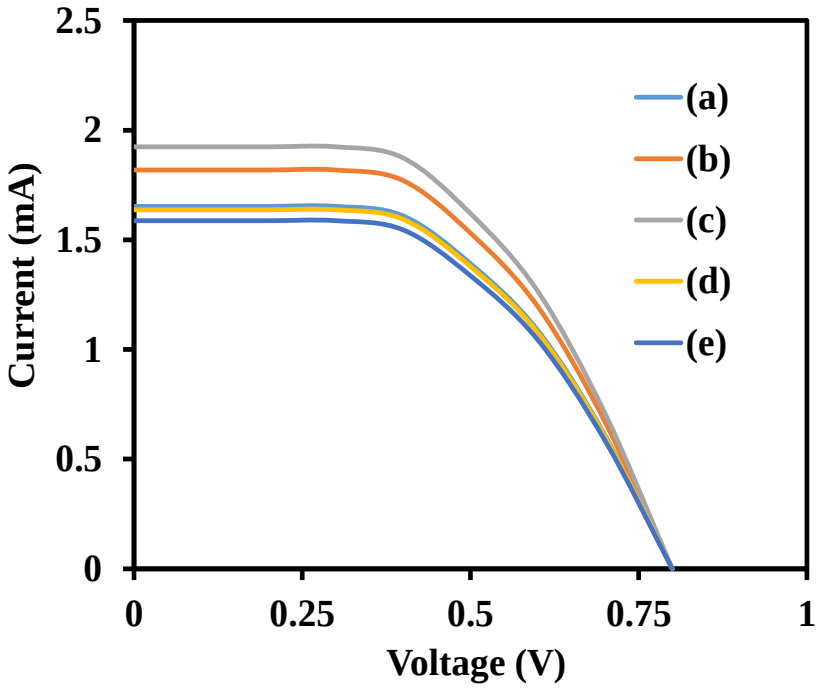

Figure 8. I-V characteristics of 20TC based PV cell with dye loading concentration (a) 1%, (b) 2%, (c) 3%, (d) 4% and (e) 5% based PV cells.

Table 3. PV parameters of 20TC based PV cells loaded with concentration ranges from 1% to 5% by an interval of 1%.

Sample	Imax (mA)	Vmax (V)	Isc (mA)	Voc (V)	FF	η(%)
1%:20TC	1.609	0.4	1.653	0.8	0.31148	4.119
2%:20TC	1.771	0.4	1.818	0.8	0.31155	4.531
3%:20TC	1.873	0.4	1.924	0.8	0.31151	4.794
4%:20TC	1.593	0.4	1.636	0.8	0.31158	4.078
5%:20TC	1.545	0.4	1.586	0.8	0.31172	3.955

Figure 9 (a-e) illustrates the current-voltage characteristics of a 3% N3 dye-loaded 20TC-based DSSC for different dye-dipping times: 1 hour, 2 hours, 3 hours, 4 hours, and 5 hours. These measurements were conducted to investigate the effect of dye-loading time on charge injection. The dye-loading time is a crucial factor that impacts the power conversion efficiency of DSSCs. Therefore, this section of the study is dedicated to analyzing the influence of N3 dye loading time on the power conversion efficiency of the optimized 3% N3 dye-loaded 20TC-based DSSC discussed in the previous section.

According to Table 4, the 3% N3 dye-loaded 20TC-based DSSC achieves the highest power conversion efficiency (5.273%) when subjected to a dye loading time of 2 hours. Beyond this optimal dye loading time, the power conversion efficiency begins to decrease. This dependence of power conversion efficiency on dye loading time can be attributed to the effect of dye-loading time on the level of dye absorption onto the TiO_2-CuO nanocomposite. A sufficiently longer dye-loading time ensures efficient and complete coverage of the material surface with dye, leading to enhanced light absorption. Additionally, the interaction between dye molecules and the TiO_2-CuO nanocomposite significantly influences charge transfer and recombination processes. An optimal dye-loading time guarantees an appropriate amount of dye molecules on the material surface, facilitating efficient charge injection from the excited dye to the TiO_2-CuO nanocomposite, minimizing charge recombination, and maximizing electron transport. Consequently, a 2-hour dye-loading time for the 3% N3 dye-loaded 20TC-based DSSC results in a higher power conversion efficiency [24, 25].

However, prolonged dye-loading times may lead to increased dye aggregation, reducing light harvesting efficiency and promoting charge recombination. Moreover, excessive dye coverage due to prolonged dye loading time can result in shading effects, where densely packed dye layers block incident photons, leading to a drop in power conversion efficiency. Therefore, in the case of higher dye loading times, the power conversion efficiency decreases due to these adverse effects.

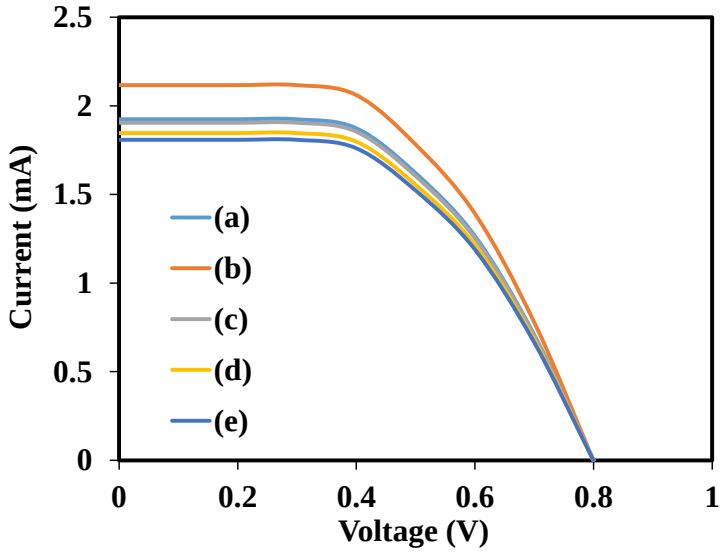

Figure 9. I-V characteristics of 3% dye loaded 20TC based PV cell for various dye-dipping time (a) 1 hour, (b) 2 hours, (c) 3 hours, (d) 4 hours and (e) 5 hours.

Table 4. PV parameters of 3% dye loaded 20TC based PV cell for various dye-dipping time ranges from 1 hour to 5 hours by an interval of 1 hour.

Sample	Imax (mA)	Vmax (V)	Isc (mA)	Voc (V)	FF	η(%)
1H:20TC	1.873	0.4	1.924	0.8	0.31151	4.794
2H:20TC	2.06	0.4	2.116	0.8	0.31153	5.273
3H:20TC	1.854	0.4	1.904	0.8	0.31159	4.746
4H:20TC	1.798	0.4	1.847	0.8	0.31151	4.602
5H:20TC	1.761	0.4	1.808	0.8	0.31168	4.508

Figure 10 (a-c) provides a comprehensive overview of the optimization of power conversion efficiency by considering three key factors: the concentration of CuO nanoparticles in the TiO_2-CuO nanocomposite, dye-loading concentration, and dye-loading time.

- In Figure 10(a), it is observed that the highest power conversion efficiency is achieved with the 20TC nanocomposite, which corresponds to a 20 wt.% loading concentration of CuO nanoparticles in the TiO_2-CuO nanocomposite. The optimization of the 20TC nanocomposite-based DSSC is the focus of this study.
- To explore the effect of dye-loading concentration, the 20TC nanocomposite system was loaded with five different concentrations of N3 dye (ranging from 1% to 5%, with a 1% interval), as shown in Figure 10(b). It is evident that the 3% N3 dye-loaded 20TC-based DSSC exhibits the highest power conversion efficiency. Thus, the optimization in this step involves the 3% N3 dye-loaded 20TC nanocomposite-based DSSC.
- Lastly, the impact of dye-loading time on power conversion efficiency was investigated and presented in Figure 10(c). It is observed that the 3% N3 dye-loaded 20TC nanocomposite-based DSSC achieves the highest power conversion efficiency when the dye loading time is set to 2 hours. Therefore, the optimization in this stage focuses on the 2-hour dye-loaded DSSC.

By experimentally optimizing three factors—namely, the concentration of CuO nanoparticles in the TiO_2-CuO nanocomposite, dye-loading concentration, and dye-loading time—this work has accomplished its main objective. The comprehensive analysis provided in Figure 10 offers valuable insights into achieving the highest power conversion efficiency in DSSCs.

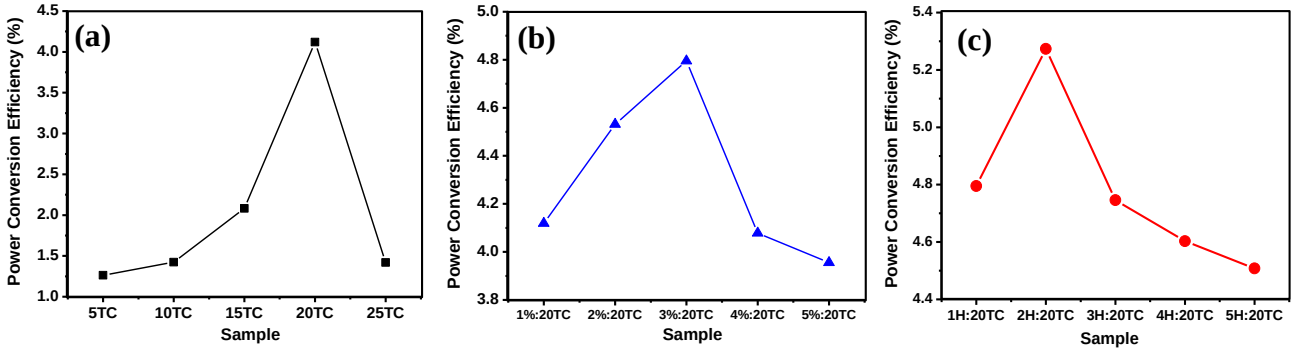

Figure 10. Variation of power conversion efficiency (a) CuO loading concentration in TiO2 composites, (b) Dye loading concentration in 20TC system and (c) Dye-dipping time of 3% dye loaded 20TC based PV cell.

IV. Conclusions

In this study, we successfully conducted an optimization process to improve the power conversion efficiency of DSSCs by investigating the effects of three key factors: the concentration of CuO nanoparticles in the TiO_2-CuO nanocomposite, dye-

loading concentration, and dye-loading time. Our results revealed that the highest power conversion efficiency was achieved when the TiO_2-CuO nanocomposite had a loading concentration of 20 wt.% CuO (20TC). This highlights the importance of optimizing the concentration of CuO nanoparticles in the composite material.

Additionally, we examined the impact of dye-loading concentration and found that a 3% N3 dye loading concentration resulted in the highest power conversion efficiency. This emphasizes the significance of optimizing the concentration of the dye used in DSSCs. Furthermore, we investigated the effect of dye-loading time and observed that a 2-hour dye loading time exhibited the highest power conversion efficiency. This indicates the importance of the duration of dye absorption in maximizing the performance of DSSCs. The successful experimental optimization of these three factors represents a significant achievement in this study. The findings provide valuable insights into enhancing the power conversion efficiency of DSSCs, which can contribute to the development of more efficient and sustainable solar energy technologies. In conclusion, the concentration of CuO nanoparticles in the TiO_2-CuO nanocomposite, N3 dye-loading concentration, and dye-loading time were identified as factors that strongly influence the power conversion efficiency of DSSCs.

V. Acknowledgment

Author is very much thankful to Vice–Chancellor, Rajiv Gandhi Prodyogiki Vishwavidyalaya (RGPV) Bhopal, State Technological University, 462033, India for providing the necessary facilities for this work.

References

[1] T. Baran, A. Visibile, M. Busch, X. He, S. Wojtyla, S. Rondinini, A. Minguzzi, A. Vertova, Copper Oxide-Based Photocatalysts and Photocathodes: Fundamentals and Recent Advances. Molecules **26**, 7271 (2021).

[2] C. Gao, Q. Han, M. Wu, Review on transition metal compounds based counter electrode for dye-sensitized solar cells. Journal of Energy Chemistry **27**, 703-712 (2018).

[3] W. Wang, X. Xu, Y. Liu, Y. Zhong, Z. Shao, Rational design of metal oxide–based cathodes for efficient dye-sensitized solar cells. Advanced Energy Materials **8**, 1800172 (2018).

[4] U. Ahmed, M. Alizadeh, N.A. Rahim, S. Shahabuddin, M.S. Ahmed, A.K. Pandey, A comprehensive review on counter electrodes for dye sensitized solar cells: A special focus on Pt-TCO free counter electrodes. Solar Energy **174**, 1097-1125 (2018).

[5] T.H. Nguyen, T.L. Nguyen, T.D.T. Ung, Q.L. Nguyen, Synthesis and characterization of nano-CuO and CuO/TiO_2 photocatalysts. Advances in Natural Sciences: Nanoscience and Nanotechnology **4**, 025002 (2013).

[6] M. Jeng, Y. Wung, L. Chang, L. Chow, Dye-Sensitized Solar Cells with Anatase TiO_2 Nanorods Prepared by Hydrothermal Method. International Journal of Photoenergy **2013**, 280253 (2013).

[7] G. Abdulnabi, A.M. Juda, Preparation and comparison performance of CuO Nanopartecles and CuO/TiO_2/Nanocomposite and application in solar cell. Journal of Kufa-Physics **15**, 1-13 (2023).

[8] M. Rokhmat, E. Wibowo, M. Abdullah, Performance improvement of TiO_2/CuO solar cell by growing copper particle using fix current electroplating method. Procedia Engineering **170**, 72-77 (2017).

[9] V.C. Martinez, A. Lopez, M.M. Gomez, Dye sensitized solar cells based on TiO_2 modified with CuO. Magazine of the Chemical Society of Peru **82**, 324-338 (2016).

[10] K. Narasimman, S. Rajakumaran, G. Vignesh, G. Glivin, M. Premalatha, A.K. Bakathavatsalam, Performance analyses of dye-sensitized solar cell with various type of electrodes and natural dyes using FTO glass. AIP Conference Proceedings **2520**, 030007 (2022).

[11] S. Shah, N.N.S. Baharun, S.N.F. Yusuf, A.K. Arof, Efficiency Enhancement of Dye-Sensitized Solar Cells (DSSCs) using Copper Nanopowder (CuNW) in TiO_2 as Photoanode. IOP Conf. Ser.: Mater. Sci. Eng. **515**, 012002 (2019).

[12] K. Nemade, P. Tekade, P. Dudhe, Strengthening of photovoltaic and supercapacitive properties of graphene oxide-polyaniline composite by dispersion of α-Al_2O_3 nanoparticles. Chemical Physics Letters **706**, 647-651 (2018).

[13] T. Salmi, M. Bouzguenda, A. Gastli, A. Masmoudi, MATLAB/Simulink Based Modeling of Photovoltaic Cell. International Journal of Renewable Energy Research **2**, 213-219 (2012).

[14] Susmita Das, Vimal Chandra Srivastava, An overview of the synthesis of CuO-ZnO nanocomposite for environmental and other applications. Nanotechnology Reviews **7**, 267-282 (2018).

[15] C.H. Ashok, K.V. Rao, Microwave-assisted synthesis of CuO/TiO_2 nanocomposite for humidity sensor application. J. Mater Sci: Mater Electron **27**, 8816-8825 (2016).

[16] A.H. Shar, M.N. Lakhan, J. Liu, M. Ahmed, M.B. Chandio, A.H. Shah, A.Hanan, I. Ali, J. Wang, Facile synthesis and characterization of mesoporous titanium oxide nanoparticles for ethanol sensing properties. Sukkur IBA Journal of Emerging Technologies **3**, 16-22 (2020).

[17] D. Renuga, J. Jeyasundari, A.S.S. Athithan, Y.B.A. Jacob, Synthesis and characterization of copper oxide nanoparticles using Brassica oleracea var. italic extract for its antifungal application. Mater. Res. Express **7**, 045007 (2020).

[18] S.C. Lee, N. Hasan, H.O. Lintang, M. Shamsuddin, L. Yuliati, Photocatalytic removal of 2,4-dichlorophenoxyacetic acid herbicide on copper oxide/titanium dioxide prepared by co-precipitation method. IOP Conf. Ser.: Mater. Sci. Eng. **2052**, 012012 (2016).

[19] H. Koo, D. Wang, Y. Yu, S. Ho, J. Jhang, M. Chen, M. Tai, Effect of Cu_2O Doping in TiO_2 Films on Device Performance of Dye-Sensitized Solar Cells. Japanese Journal of Applied Physics **51**, 10-18 (2012).

[20] M. Dhonde, K. Sahu, V.V.S. Murty, Cu-doped TiO_2 nanoparticles/graphene composites for efficient dye-sensitized solar cells. Solar Energy **220**, 418-424 (2021).

[21] T. Raguram, K.S. Rajni, Synthesis and characterisation of Cu-Doped TiO_2 nanoparticles for DSSC and photocatalytic applications. International Journal of Hydrogen Energy **47**, 4674-4689 (2022).

[22] T.P. Chou, Q. Zhang, G. Cao, Effects of Dye Loading Conditions on the Energy Conversion Efficiency of ZnO and TiO_2, Dye-Sensitized Solar Cells. J. Phys. Chem. C **111**, 18804-18811 (2007).

[23] A.F. Kamil, H.I. Abdullah, A.M. Rheima, Fabrication of Dye-sensitized Solar Cells and Synthesis of $CuNiO_2$ Nanostructures Using a Photo irradiation Technique. Journal of Nanostructure **12**, 144-159 (2022).

[24] S. Aksoy, K. Gorgun, Y.Y. Caglar, M. Caglar, Effect of Loading and Standbye Time of the Organic Dye N719 on the Photovoltaic Performance of ZnO Based DSSC. Journal of Molecular Structure **3**, 1189 (2019).

[25] Md. Khalid Hossain, M. Firoz Pervez, M.N.H. Mia, A.A. Mortuza, M.S. Rahaman, M.R. Karim, Jahid M.M. Islam, Farid Ahmed, Mubarak A. Khan, Effect of dye extracting solvents and sensitization time on photovoltaic performance of natural dye sensitized solar cells. Results in Physics **7**, 1516-1523 (2017).